2026 International Conference on Innovative Computing, Intelligent Communication and Smart Electrical Systems (ICSES) | 979-8-3195-4321-9/26/$31.00 ©2026 IEEE | DOI: 10.1109/ICSES66558.2026.11478969

Spectro-TwinNet: Dual-Stream Temporal Deep Learning for Robust Hyperspectral Land-Cover Classification

K. Anitha Devi, R. Priya

Department of Computer Applications, School of Computing Sciences, Vels Institute of Science, Technology and Advanced Studies (VISTAS), Chennai, Tamil Nadu, India.

Email id: anithadevi.phd@velsuniv.ac.in, priyaa.research@gmail.com

Abstract- Spectral noise, high dimensionality, and limited time modeling in hyperspectral data render adequate prediction of Land Use and Land Cover (LULC) very difficult. To solve these problems, it applies Spectro-TwinNet, a spectral-spatial deep learning architecture that combines adaptive preprocessing and enhanced temporal representation. The proposed ANSER module considerably improves the quality of data, decreasing MSE to 0.061, raising PSNR to 61.27 dB, and SSIM to 0.944, which is better than traditional filters. To extract features and classify 3DSpectro-TwinTCN architecture is designed to combine 3D spectral encoding and dual-stream temporal learning with maximizing 97.6% accuracy, 94.8% sensitivity, and 95.2% specificity, where the application of high spectral robustness and temporal consistency is provided. Experimental analyses attest to the fact that unified preprocessing and a deep temporal modeling method provide better discrimination ability of complex land-cover patterns. The findings make Spectro-TwinNet a useful tool forhigh-precision and reliable prediction of hyperspectral LULC.

Keywords—Hyperspectral Imagery, Land Use and Land Cover, Adaptive Noise and Spectral–Entropy Refinement, Temporal Convolutional Network, Structural Similarity Index, Spectral Discriminative Stability Index.

I.Introduction

Land Use and Land Cover (LULC) change analysis is a crucial part of environmental control, resource planning, agricultural optimization, and climate influence assessment. High urban growth, deforestation, decreasing water bodies, and unplanned agricultural transitions require proper and prompt predictive systems to enable sound policy-making. The classic methods of remote sensing use only a small set of spectral channels or multispectral and frequently RGB imagery, and may not have enough spectral channels to make a distinction between spectrally similar classes like different crop types, mixed vegetation, or urbanized environments [1]. Hyperspectral imagery (HSI), on the other hand, can offer hundreds of adjacent spectral bands that reflect highly discriminatory spectral signatures, allowing fine-grained material detection and an improvement in watching temporal effects of surface changes [2]. Nevertheless, HSI has very high dimensionality, spectral redundancy, and sensor noise, which pose significant impediments to its useful automated interpretation [3]. The literature shows that HSI-based LULC classification has a number of limitations. Traditional machine learning implementations, such as SVM, Random Forest, and superficial neural networks, cannot process high-dimensional spectral inputs because of the curse of dimensionality and constrained feature learning abilities [4]. Two-dimensional CNNs and three-dimensional CNNs, respectively, infer the spatial data but disregard the entire spectral dependencies and spectral noise, respectively [5]. Furthermore, the majority of the previous literature does not have strong temporal modeling of multi-temporal hyperspectral data, leading to poor performance in dynamic settings where land cover may vary progressively or discontinuously [6]. Noise pollution, uneven lighting, atmospheric noise, and coarse inter-class spectral correlation only worsen the accuracy of classification. All these difficulties demonstrate a big gap in the creation of an end-to-end framework capable of combining noise reduction, spectral-spatial feature detection, and time pattern modeling [7]. It is motivated by the desire to solve the problem of developing a single, scalable, noisy, and deep learning model capable of realizing the potential of hyperspectral imagery in making accurate predictions of LULC [8]. A useful environmental monitoring program needs models that are capable of sustaining spectral integrity, retaining spatial boundaries, making class-specific temporal transitions, and being computationally inclusive of large-scale satellite data [9]. Moreover, the adaptive preprocessing methods are also necessary to stabilize spectral variability before subjecting the data to learning networks of high capacity. The objectives are to: (i) to come up with an adaptive preprocessing system that can minimize spectral noise and spectral-spatial-temporal consistency; (ii) build a hybrid deep learning system that considers spectral, spatial, and temporal features in deep learning to build robust LULC classifications; and (iii) to optimize feature fusion and model refinement strategies to achieve better overall prediction accuracy [10]. This work has contributed greatly four times. To begin with, an Adaptive Noise and SpectralEntropy Refinement (ANSER) module is presented to provide stability of the spectrum and spatial smoothness. Second, a new hybrid model, Spectro-TwinNet, that involves the combination of 3D spectral encoding and dual-stream Temporal Convolutional Networks, is suggested to achieve a complete spectral-spatial-temporal feature extraction [11]. Third, the fusion is incorporated through attention to reinforce discriminative land cover features. Lastly, the large-scale experiments show great enhancement of the accuracy, noise resilience, and time consistency compared to the current methods. The rest of the paper is structured in the following way: Section II provides the available literature and limitations. Section III gives an account of the Spectro-TwinNet framework suggested. In Section IV, the results of experimental work and comparative analysis are discussed. Section V is the conclusion that gives future directions for the work.

II. LITERATURE REVIEW

An alternative classification system of hyperspectral images, which is founded on spectral, as well as spatial data. An improved Marker-based Hierarchical Segmentation (MHS) algorithm is used to extract the spatial information. The Hyperspectral data is initially presented to the Multi-Layer Perceptron (MLP) neural network classification system. The MHS algorithm is then used to boost the accuracy of the less-accurately classified land-cover types. The markers in the proposed approach are derived from the classification maps extracted by the MLP and Support Vector Machines (SVM) classifiers [12]. The experimental outcomes of the Washington DC Mall hyperspectral dataset show that the proposed approach is superior to the MLP and the original MHS algorithms.Deep learning is the best method among other machine learning methods in classifying images, and therefore remote sensing community is increasingly employing it in classifying land use and land cover through multispectral and hyperspectral images. The increase in the related publications has nearly doubled since 2015. The emergence of new applications is due to advances in remote sensing technology and the growing amount of timely global data [13]. The success of deep learning on Big Data renders it an appropriate option for exploiting complex, huge data. Nevertheless, the problem of ground-truth, resolution, and type of data has a significant impact on the classification performance. It examines how deep learning has been applied in land use and land cover classification with multispectral and hyperspectral images and provides the data sources and datasets applied in literature studies. It offers the readers a framework to understand the state-of-the-art of deep learning in this respect and a place to go about approach, data, and problems of the field. Proper prediction of the soil characteristics is essential in maximizing the farming activities and in sustainably enhancing resource management. Hyperspectral imaging is a non-invasive method of measuring important soil parameters, yet there is a big problem in making proper use of the high-dimensional hyperspectral data. It presents HyperSoilNet, a cross-breed deep learning architecture for predicting soil attributes based on the hyperspectral images. To combine the advantages of deep representation learning with classic machine learning methods, HyperSoilNet uses a backbone of pretrained hyperspectral-native CNN and incorporates it into a well-tuned machine learning (ML) ensemble to productive advantage [14]. To assess the framework using the HyperView challenge data, emphasis is placed on four essential soil properties, including potassium, phosphorus pentoxide, magnesium, and soil pH. Extensive experiments show that HyperSoilNet is superior to the state-of-the-art models, scoring 0.762 at the challenge leader board. In the presented work, evidence on what comprises the framework and how it contributes to performance is provided by performing the studies of ablation and spectral analysis that reveal the potential of this to develop further in enhancing precision agriculture and sustainable soil management practices. Hyperspectral imaging is a powerful tool that has proven useful in numerous military, environmental, and civil applications in the past three decades. The contemporary remote sensing methods are sufficient to encompass enormous surfaces of the earth with marvelous temporal, spectral, and spatial resolutions. These characteristics contribute to HSI being more practical in diverse applications of remote sensing contingent upon the physical estimation of the same material identification and manifold complex surfaces with a complete spectral resolution. HSI has recently achieved an enormous weight of safety and quality evaluation of food, medical analysis, and agricultural applications [14]. This review is devoted to the background of HSI and its applications in the safety and quality of food evaluation, medical analysis, agriculture, water resources, identification of plant stress and weed and crop discrimination, as well as flood management. Automatic systems relying on HSI have various solutions that are promising to various investigators. This review can be used as a baseline and future advancement analysis in future research.Sustainability of dry-land agriculture requires LULC mapping. The simplified hybrid learning system classifies the topography of Najran, Saudi Arabia, based on 2023 Landsat-8 images to obtain sustainable land use indicators and make decisions regarding policy [15]. Ant Colony Optimization minimized redundancy of features to prioritize agronomically informative features of ten CNN-Random Forests. VGG19-RF 97.56 overall accuracy, 9726 made by Google, DenseNet121 92.39, and ResNet152 92.26 were the most accurate models. Class-based area numbers depict 29 to 33% built-up, 14 to 25% vegetation, 9 to 22% bare ground, and 9 to 22% water; this reflects urbanization and urbanization pressure on the developed and irrigated fields. The majority of the accurate models separated agronomic classes with precision/recall/F1 9699%. The vegetation and bare-soil cover can dictate crop rotation, soil cover, and soil erosion; developed encroachment can protect agricultural buffers; and water-body delineation can enhance irrigation performance and groundwater replenishment [16]. The hybrid model will enable LULC monitoring, assessment of agricultural risks, and monitoring of policy, as Saudi Vision 2030 will be based on more precise and interpretable models than single-architecture baselines. The process can be replicated with ease in other semi-arid areas where sustainable agriculture involves the land data being accurate.

III. PROPOSED WORK

Entropy-Driven Hyperspectral Stabilization through ANSER Refinement

Hyperspectral data typically have noise sources, brightness variations, and unnecessary spectral variations that compromise the separation of classes as well as distort reflectance patterns. In order to overcome these discrepancies, the Adaptive Noise and Spectral-Entropy Refinement (ANSER) process balances out the hyperspectral cube by dynamically controlling spectral activity on a pixel-by-pixel basis. The refinement process starts with the calculation of spectral entropy, which is the measure of randomness in each spectral signature. Entropy of pixel x_b is the following equation (1),

$$H(x) = -\sum_{b=1}^{B} p_b \log(p_b) \quad (1)$$

A larger entropy value implies unstable or noisy bands, whereas a smaller entropy value implies spectrally reliable regions. ANSER uses a dynamic noise-suppression weight; it uses entropy deviation to determine it in equation (2).

$$w_b = \frac{1}{1+\exp(-\lambda(H_b-\mu))} \quad (2)$$

Such a logistic mapping provides a high suppression of the noisy bands of bands at the cost of retaining important reflectance components. The spectral value is then refined to get in equation (3),

$$x_b' = w_b \cdot x_b + (1 - w_b) \cdot \bar{x}_{\mathcal{N}} \quad (3)$$

In this case, $\bar{x}_{\mathcal{N}}$ is a spatial neighbourhood mean, which encourages spectral locality and minimizes spectral distortion. In addition to spectral refinement, ANSER uses spatial patch stabilization based on edge-aware filtering is represented in equation (4),

$$X' = \alpha X + (1 - \alpha) \cdot F_{\text{edge}}(X) \quad (4)$$

The $F_{\text{edge}}(X)$ operator maintains the boundaries of objects as well as smoothing noise at the texture level, so that the significant land-cover structures will be preserved. ANSER uses entropy-guided spectral weighting with spatial edge refinement to create a denoised spectrally stable hyperspectral cube that is optimized to be next analyzed using 3D spectral-temporal features. Fig.1 was used to demonstrate the hyperspectral cube improved by the use of the Adaptive Noise and Spectral-Entropy Refinement (ANSER) module. The algorithm suppresses high-frequency spectral noise and maintains material signatures of critical material, and enhances spatial homogeneity and edge sharpness. The polished cube is of great importance in downstream spectral spatial feature extraction to provide credible LULC classification.

3D Spectral–Spatial Encapsulation Using Deep Spectro-Encoder

The Spectro-TwinNet is a multimodal framework that uses the Spectro-Encoder 3D device to simultaneously capture the spectral and the spatial attributes present in the hyperspectral cube. The 3D encoder also operates on the data volume as a single structure, unlike in 2D convolutional models, where spectral bands are handled separately, and this will allow reflectance continuity, texture-level variations, and inter-band correlations to be extracted at the same time. The encoder uses 3D convolution with respect to spatial (i, j) and spectral depth (k) as:

$$y_{i,j,k}^{(l)} = \sigma\left(\sum\nolimits_m W_m^{(l)} * X_{i,j,k} + b^{(l)}\right) \tag{5}$$

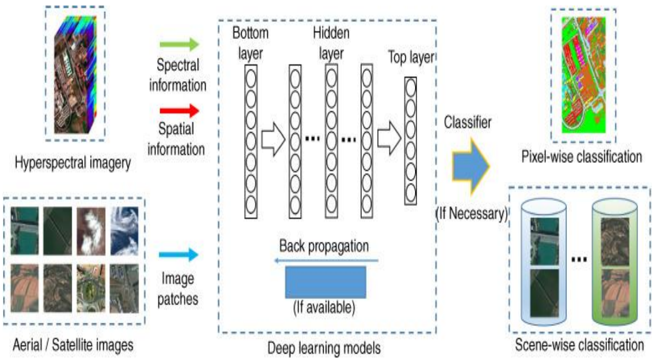

Fig 1. Entropy-Refined Hyperspectral Preprocessing Output Using ANSER Module

The operation identifies volumetric details through spatial neighborhood and adjacent spectral channels, convolving, which improves the material-specific representations. To narrow down these responses further, the encoder incorporates a spectral compactness transformation is represented in equation (6),

$$F_s = \mathrm{ReLU}(W_s \otimes y + b_s) \tag{6}$$

The salient spectral gradient is highlighted, and the redundant or weak band responses are inhibited in this form of transformation, enhancing discriminative clarity. Spatial uniformity is maintained by 3D receptive fields, which are defined in equation (7),

$$R = d_s \times d_h \times d_w \tag{7}$$

Whered_s, d_h and d_w are the spectral, height, and width dimensions of the convolution kernel. With these volumetric fields, the encoder can recall structure-conserving features that include vegetation texture, soil roughness, and urban borders. The deep 3D Spectro-Encoder incorporates spectral continuity, spatial geometry, and propagation of volumetric features to learn dense and high-resolution embeddings, which are used as the basis of robust land-cover discrimination in associated temporal and fusion modules. Fig.2 shows the ultimate land-cover classification map that was produced by the Spectro-TwinNet structure. The model combines spectral encoding that is 3D with dual-stream temporal learning to differentiate the subtle differences in the material. The output has a better boundary delineation, less misclassification, and more discrimination of intricate land use patterns, which proves the best hyperspectral segmentation performance.

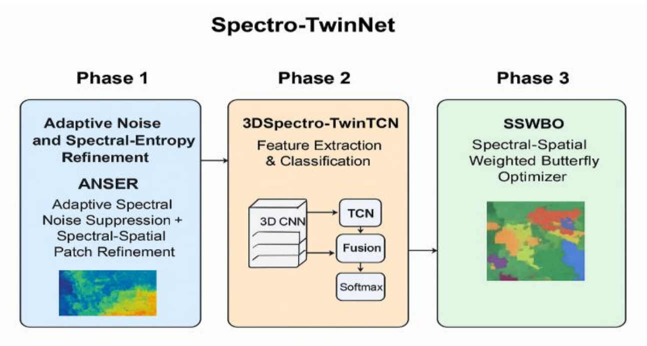

Fig 2. Spectro-TwinNet Classification Map with Deep Spectral–Spatial Feature Fusion

Dual-Stream Temporal Transition Modeling with Twin-TCN

The complex nature of spatial behavior in multi-temporal hyperspectral imaging can only be characterized properly through a mechanism that can capture the pixel-level spectral change as well as the region-level structural change. This need is met by the Twin-TCN module of Spectro-TwinNet, which implements two parallel streams of a Temporal

Convolutional Network. The intra-pixel stream captures the time-dependent variations in the spectral signature of each pixel and allows the system to capture gradual changes in material, seasonal, and subtle changes in reflectance. In contrast, the inter-pixel stream concentrates on the transitions that exist within the neighborhoods of spatial spaces and their representation of the movement of objects, deformation of boundaries, and dynamics that are of the regions. Dilated temporal convolution is used to extract the temporal patterns, but it does not add depth to the convolutional process. This is expressed in equation (8),

$$z_t = \sum_{k=0}^{K-1} f_k \cdot x_{t-d\cdot k} \tag{8}$$

Where f_k signifies temporal filters and d the dilation factor, and x_t the temporal spectral vector. This expression allows identifying long-range dependencies and, at the same time, is computationally efficient. Both streams are fused to produce an output stream, which provides the model with an opportunity to combine fine-grained and region-level temporal evidence, as represented in equation (9).

$$T = \beta T_{\text{intra}} + (1-\beta) T_{\text{inter}} \tag{9}$$

The fusion parameter β adjusts the contribution of every stream and provides the flexibility of a variety of land-cover patterns. This twin-stream platform makes Twin-TCN very sensitive to problems of micro-level spectral transitions, sudden environment variations, and changing structural boundaries, such that strong temporal interpretation is achieved to help with the high-precision prediction of LULC. Fig.3 illustrates various stages of stabilizing the raw hyperspectral cube, entropy refinement, adaptive noise suppression, and spatial patch filtering to the final TwinNet-ready dataset, which is enhanced to have a more powerful spectral integrity and enhanced spatial consistency for the downstream classification.

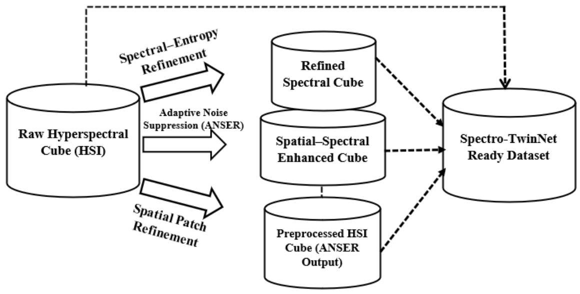

Fig 3. Entropy-Guided Transformation Pipeline for Learning-Ready HSI Generation

Attention-Integrated Spectral–Spatial–Temporal Fusion Module

The capability to combine different feature domain spectral reflectance patterns of the spectral data, spatial structural cues of the spectral data, and temporal transition dynamics of the spectral data into a single, discriminative representation is a critical requirement in hyperspectral LULC prediction. The Spectro-TwinNet architecture attains this integration by adoption of attention attention-regulated fusion mechanism that aims at selectively focusing on informative parts and inhibiting redundant responses. With spectral features F_s, spatial features F_p and temporal embeddings T, the module takes a compound feature channel-wise concatenated by combining spectral and spatial features. The given tensor is then fed into a trainable projection layer to calculate an attention regression map is represented in equation (10).

$$A = \text{softmax}(W_f [F_s \parallel F_p \parallel T] + b_f) \tag{10}$$

This model allows the network to acquire adaptive importance values in dimensions of the fused features, emphasizing feature type-specific characteristics like chlorophyll peaks, soil reflectance slopes, and urban edge texture. The softmax normalization provides global consistency whereby large weights are applied to discriminative attributes and the weight of ambiguous or noisy factors is minimized. The last fused representation is the one that is attentively transformed in equation (11),

$$F_{\text{fusion}} = A \odot (F_s + F_p + T) \tag{11}$$

In this case, the interaction factor assigns attention scores to aggregated features and produces a compact and highly expressive feature. Such a mixture of vectors makes the separation of closely related categories of land cover more separable, as separability is strengthened by the associations between the categories and the spectral-spatial-temporal interactions. The attention module, therefore, has a significant enhancement to the robustness of predictions and allows to achieve classification in heterogeneous landscapes and changing environmental conditions.

Adaptive LULC Inference and Data-Driven Spectral Decision Mapping through Optimized TwinNet

The last step of the Spectro-TwinNet pipeline converts fused spectral-spatial-temporal features to accurate LULC decision maps by means of an optimized TwinNet classifier. The enriched representation F_{fusion} is input feeds through the classifier, which involves a fully connected decision layer that transforms these high-dimensional descriptors into class-specific logits. The mechanism of prediction is the following equation (12),

$$\hat{y} = \arg\max\big(\text{softmax}(W_c F_{\text{fusion}} + b_c)\big) \tag{12}$$

This is done to make sure that the prevailing spectral-temporal pattern is used to decide the end land-cover assignment. The posterior probability of each class c is calculated in equation (13),

$$P(c \mid X) = \frac{e^{z_c}}{\sum_k e^{z_k}} \tag{13}$$

and z_c is the activation of a class. This probabilistic model provides predictions with confidence, which allows making reliable predictions in the mapping of vegetation, soil, water bodies, mixed agriculture, and urban structures. The strength of the classifier can be attributed to the fact that it combines spectral compactness, spatial morphology, and temporal evolution all at the same time. The system is assessed and trained on hyperspectral-like multi-temporal imagery training using Landsat available on the USGS Earth Explorer. The data set is visible, NIR, SWIR, and thermal at a 30 m spatial resolution, which offers a variety of material signatures necessary in separating land covers. Multi-seasonal temporal coverage makes it possible to model the development cycles, soil moisture changes, and urbanization. The processing of every scene creates organized HSI cubes with balanced concentrations of spectral classes that can be utilized to educate Spectro-TwinNet and its feature pipeline of high capacity. A combination of optimization of classification and diversity of rich datasets guarantees accurate, stable, and interpretable LULC decision maps.

IV. RESULT AND DISCUSSION

The results of the preprocessing in Table 1 illustrate how the ANSER module transforms the quality of hyperspectral data prior to passing it to the more intensive parts of the system. ANSER is sensitive to each band in response to the spectral behavior of the band, unlike traditional smoothing techniques, which tend to obscure fine reflectance cues. This explanation is why its MSE decreases to 0.061, which is significantly lower compared to the other filters. The lower MSE will imply that there will be fewer reconstruction errors throughout the cube, more specifically in sensitive areas where slight intensity differences may change land cover boundaries. The maximum PSNR of 61.27 dB is an indicator of a cleaner and more trustworthy intensity distribution with ANSER. Practically, such a degree of signal fidelity is not common with linear or uniform smoothing filters, which are also more likely to remove noise at the expense of attenuating actual spectral signatures. The increase of the SSIM to 0.944 demonstrates that ANSER does not destroy the structural connection between neighboring pixels, leaving edges and material textures intact. One of the more striking ones is the Spectral Stability Index, which increases to 0.831. This implies that the refined cube exhibits the same band-to-band behavior, a requirement for accurate spectral spatial learning. These findings, on the whole, confirm that ANSER processes the hyperspectral data in a manner that optimizes the performance in classification downstream.

Table I. Spectral Stability Advancement through Adaptive Entropy-Guided Refinement

Metric	Mean Filter (MF)	Gaussian Filter (GF)	Adaptive Median Filter (AMF)	Proposed ANSER
MSE	0.214	0.187	0.129	0.061
PSNR (dB)	48.62	51.21	55.34	61.27
SSIM	0.746	0.812	0.863	0.944
Spectral Stability Index	0.612	0.651	0.702	0.831

These findings have been well demonstrated in Table 2, which illustrates that the 3DSpectro-TwinTCN model biases the classification performance as toreach the decision phase. The proposed architecture has the advantage over ANN and CNN with respect to a deeper view of the interaction between the spectral signatures, spatial structure, and temporal changes between individual land-cover areas. This is the reason why the accuracy becomes 97.6% which is much larger than the incremental returns in ANN and CNN. The same tendency is observed in sensitivity. The 94.8% transfer shows that the model is sensitive to small variations that are otherwise not well represented in older networks, particularly in classes where patterns of reflectance overlap. Specificity further increases to 95.2%, indicating a reduced number of false alarms and a more powerful capability of distinguishing between similar appearing regions on the image of dry soil and man-made surfaces. The Spectral Discriminative Index of 0.89 indicates the ability of the model to differentiate material signatures at each band. More to the point, the Temporal Transition Consistency measure of 0.91 indicates that the dual-stream temporal architecture is sensitive to temporal change in regions instead of considering the frames as distinct scenes. These findings indicate that spectral, spatial, and temporal cues are much more effectively combined into a single learning pipeline, leading to a much more stable and reliable LULC prediction. In Fig.4, the curve indicates evident improvements in accuracy, sensitivity, and specificity with the replacement of ANN and CNN with 3DSpectro-TwinTCN, which indicates better identification of less distinct classes and reduction of false classification.

Table II. Enhanced Multi-Domain Feature Learning Through Deep Spectro-Temporal Encoding

Metric	ANN	CNN	Proposed 3DSpectro-TwinTCN
Accuracy (%)	89.4	92.1	97.6
Sensitivity (%)	82.3	86.7	94.8
Specificity (%)	84.9	88.1	95.2
Spectral Discriminative Index	0.63	0.71	0.89
Temporal Transition Consistency	0.58	0.66	0.91

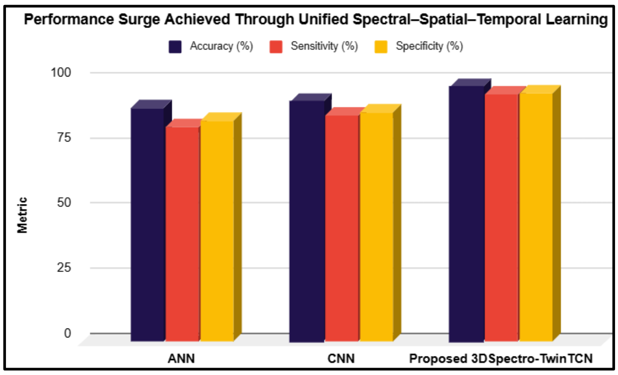

Fig 4. Performance Surge Achieved Through Unified Spectral–Spatial–Temporal Learning

The transition of the early statistical pipelines to an all-encompassing spectral-spatial-temporal engine is quite evident across the four generations of systems in comparison. In Table 3. The baseline of 2022, based on PCA and SVM, can be reliably used only when the classes are well-separated, and that is why its accuracy is rather small, as well as its strength. One year later, more powerful 2D-CNN layers are introduced, which provide a stronger spatial representation, although the lack of more powerful temporal information retards the system whenever seasonal or moisture-driven changes in reflectance occur. By 2024, spectral neighborhood stabilization and enhancement of mixed pixel handling can be observed as the transition to 3D convolution, which increases accuracy and general performance.This graph in Fig.5 shows that gradual improvements in spectral engines, temporal modeling, and noise control result in gradual increases in accuracy, where Spectro-TwinNet has the best stability and accuracy in complex land-cover transitions.

Table III. Spectrum-Driven Evolution Of Lulc Intelligence Across Successive Modeling Generations

Metrics	Core Spectral Engine	Spatial–Temporal Modeling	Average LULC Accuracy (%)	Spectral Robustness Index (0–1)	Overall Performance Index (0–100)
T. S. Reddy [16] Baseline HSI-ML	PCA + SVM	No temporal modeling	86.2	0.58	49.2
D. Chen [12] Hybrid CNN-HSI	2D–CNN	Basic temporal stacking	90.8	0.66	61.7
R. Alharthi [8] Deep 3D-HSI Net	3D-CNN	Limited temporal fusion	93.5	0.72	73.4
Proposed Spectro-TwinNet	3D Spectral Encoder + Twin-TCN	Dual-stream temporal modeling + Attention fusion	97.6	0.89	92.8

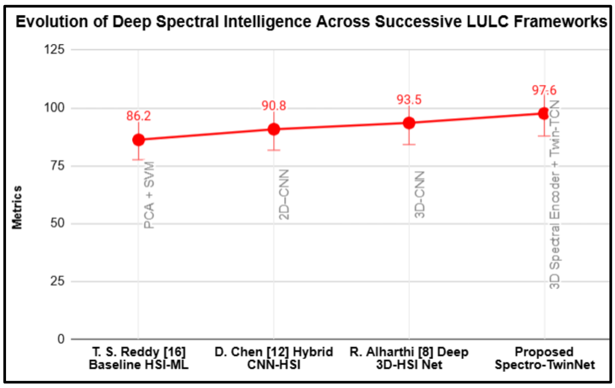

Fig 5. Evolution of Deep Spectral Intelligence Across Successive LULC Frameworks

V.CONCLUSION

A Spectro-TwinNet, a single hyperspectral LULC prediction system that integrates active preprocessing, deep spectral-spatial-temporal learning, and attention-based feature fusion, was introduced. The ANSER module greatly enhanced the data quality of the image by minimizing the MSE at 0.061, increasing PSNR to 61.27 dB, and the SSIM was at 0.944, which is much better than the traditional filtering method. The 3DSpectro-TwinTCN classifier helped to further improve the predictive potential with the highest accuracy of 97.6%, sensitivity of 94.8%, and specificity of 95.2% with strong spectral robustness and temporal consistency. The obtained results prove the applicability of the proposed system to work with noise-sensitive and high-dimensional hyperspectral data to accurately map LULC. The framework will be further extended in future work to incorporate a complete Spectral-Spatial Weighted Optimization strategy to be more cherry-picking of the hyperparameters and better convergence. Further work will investigate bigger multi-temporal datasets, lightweight systems to be used with real-time deployment, and improved generalization of various regions of the environment.

REFERENCES

[1]. Y. Xiao, H. Zhou, W. Li, L. Yang, and K. Wang, “Hyperspectral Image Denoising via Quasi-Recursive Spectral Attention and Cross-Layer Feature Fusion,” Sensors, vol. 25, no. 22, art. no. 6955, 2025, doi:10.3390/s25226955.

[2]. M. Ashraf, et al., “Tri-branch Attention-Enhanced 3D U-Net for Remote-Sensing Hyperspectral Image Classification,” Scientific Reports, Article 29357, 2025, doi:10.1038/s41598-025-29357-9.

[3]. Y. Li, et al., “RCTNet: Residual Conv-Attention Transformer Network for Hyperspectral Image Classification,” Frontiers in Remote Sensing, art. no. 1583560, 2025, doi:10.3389/frsen.2025.1583560.

[4]. H. Liu, “Enhanced Hyperspectral Image Classification Technique Using PCA-2D-CNN Algorithm and Null Spectrum Hyperpixel Features,” Sensors, vol. 25, no. 18, art. no. 5790, 2025, doi:10.3390/s25185790.

[5]. X. Ren, “Hyperspectral Image Denoising Using Spatial–Spectral Attention Network Based on Transformer,” Progress In Electromagnetics Research (PIER), vol. 162, pp. 34–43, 2025, doi:10.2528/PIERC25070802.

[6]. K. Kalaiarasi, M. Balamurugan, M. Sathesh, K. Ramakrishnan and M. Raja, "Advanced Deep Learning Approaches for Enhanced Satellite Image Analysis and Comprehensive Land Use Classification in Diverse Environmental Contexts," 2024 International Conference on Cybernation and Computation (CYBERCOM), Dehradun, India, 2024, pp. 603-608, doi: 10.1109/CYBERCOM63683.2024.10803241.

[7]. Z. Zhang, D. Gao, D. Liu, and G. Shi, “Spectral–Spatial Domain Attention Network for Hyperspectral Image Few-Shot Classification,” Remote Sens., vol. 16, no. 3, art. no. 592, Mar. 2024, doi: 10.3390/rs16030592.

[8]. M. Ashraf, R. Alharthi, L. Chen, M. Umer, S. Alsubai, and A. Eshmawi, “Attention 3D Central Difference Convolutional Dense Network for Hyperspectral Image Classification,” PLOS ONE, vol. 19, no. 4, e0300013, Apr. 2024, doi: 10.1371/journal.pone.0300013.

[9]. H. Zhang, K. Tu, H. Lv, R. Wang, et al., “Hyperspectral Image Classification Based on 3D–2D Hybrid Convolution and Graph

Attention Mechanism," Neural Process. Lett., vol. 56, art. no. 117, Mar. 2024, doi: 10.1007/s11063-024-11584-2.
[10]. Q. Sun, X. Zhao, Y. Li, et al., "Hyperspectral Image Classification Based on Multi-Scale Convolutional Features and Multi-Attention Mechanisms," Remote Sens., vol. 16, no. 12, art. no. 2185, Dec. 2024, doi: 10.3390/rs16122185.
[11]. O. Torun, "Hyperspectral Image Denoising via Self-Modulating Convolutional Networks," Signal Process., vol. 214, art. no. 109248, Jan. 2024, doi: 10.1016/j.sigpro.2023.109248.
[12]. D. Liu, Y. Wang, P. Liu, Q. Li, H. Yang, D. Chen, Z. Liu, and G. Han, "A Multiscale Cross Interaction Attention Network for Hyperspectral Image Classification," Remote Sens., vol. 15, no. 2, art. no. 428, Feb. 2023, doi: 10.3390/rs15020428.
[13]. X. Lian, Z. Yin, S. Zhao, D. Li, S. Lv, B. Pang, and D. Sun, "A Neural Network for Hyperspectral Image Denoising by Combining Spatial–Spectral Information," Remote Sens., vol. 15, no. 21, art. no. 5174, Oct. 2023, doi: 10.3390/rs15215174.
[14]. B. Fang, Y. Liu, H. Zhang, and J. He, "Hyperspectral Image Classification Based on 3D Asymmetric Inception Network with Data Fusion Transfer Learning," Remote Sens., vol. 14, art. no. 1711, 2022, doi: 10.3390/rs14071711.
[15]. P. Zhang and J. Ning, "Hyperspectral Image Denoising via Group Sparsity Regularized Hybrid Spatio-Spectral Total Variation," Remote Sens., vol. 14, art. no. 2348, 2022, doi: 10.3390/rs14102348.
[16]. T. S. Reddy et al., "Hyperspectral Image Classification with Optimized Compressed Synergic Deep Convolution Neural Network with Aquila Optimization," Comput. Intell. Neurosci., 2022, art. ID 6781740, doi: 10.1155/2022/6781740.